First charged tracks reconstructed with Timepix4 ASIC

K. Akiba[a], M. van Beuzekom[a], V. van Beveren[a], W. Byczynski[b,c],
V. Coco[b], P. Collins[b], E. Dall'Occo[d], R. Dumps[b], T. Evans[e],
R. Geertsema[a], E.L. Gkougkousis[b], M. Halvorsen[b], B. van der Heijden[a],
K. Heijhoff[a], E. Lemos Cid[f], T. Pajero[g], D. Rolf[d], H. Schindler[b]

[a] *Nikhef, Science Park 105, 1098 XG Amsterdam, the Netherlands*
[b] *CERN, 1211 Geneve, Switzerland*
[c] *Tadeusz Kosciuszko Cracow University of Technology, Cracow, Poland*
[d] *TU Dortmund, Otto-Hahn-Strasse 4, 44227 Dortmund, Germany*
[e] *Department of Physics and Astronomy, University of Manchester, Manchester, United Kingdom*
[f] *Instituto Galego de Fisica de Altas Enerxias (IGFAE), Universidade de Santiago de Compostela, Santiago de Compostela, Spain*
[g] *Department of Physics, University of Oxford, Denys Wilkinson Bldg., Keble Road, Oxford, OX1 3RH, United Kingdom*

Abstract

The design of a detector system comprised of four silicon sensors bump-bonded to Timepix4 ASICs is described together with its data acquisition system, operational infrastructure, and dedicated software. The spatial and temporal performance of the system are assessed with a 180 GeV/c mixed hadron beam at the CERN SPS and reported in detail. Particle tracks are reconstructed using time-space measurements from the four detector planes. The spatial hit resolution is assessed to be (15.5 ± 0.5) µm and (4.5 ± 0.3) µm for 100 µm and 300 µm thick sensors, respectively. The timestamps from the detectors are also measured with fine precision, yielding time resolutions of (452 ± 10) ps, (420 ± 10) ps, (639 ± 10) ps, (631 ± 10) ps for the two 100 µm and two 300 µm thick sensors respectively. These measurements are combined to a track time resolution of (340 ± 5) ps.

Keywords: Solid state detectors, Particle tracking detectors, Timing detectors

---

Preprint submitted to Nuclear Instruments and Methods A *October 5, 2022*

1. Introduction

Future experiments in high energy physics will require timing measurements of the order of 10 ps in addition to the state-of-the-art spatial measurements. The main motivation is to cope with the high occupancy at hadron colliders operating at a high number of collisions per bunch crossing, by separating tracks from different quasi-simultaneous collisions [1]. The Timepix Application Specific Integrated Circuit (ASIC) family has previously been employed in the reconstruction of charged particle trajectories [2, 3, 4, 5], in particular as an R&D platform for sensors, ASICs and other detector components used for the upgrades of the LHCb experiment. Timepix4 [6] is a novel ASIC designed for performing both temporal and spatial measurements with 195 ps bin width and $55 \times 55\,\mu\text{m}^2$ pixel size. Its increased precision enables the use of spatial and temporal information in a 4D-tracking approach, and it will play a pivotal role in the R&D efforts for the next generation of experiments.

In this paper the design of a single arm four-plane telescope based on the Timepix4v1 ASIC is described together with the data acquisition system, operational infrastructure and dedicated software. This is a first step towards a two arm telescope with at least eight planes with the final version of Timepix4 ASIC, targeting a spatial resolution of 2 μm or better and a temporal resolution of O(30) ps. Finally, the spatial and temporal performances are assessed using a 180 GeV/c mixed hadron beam at the SPS H8 beam line facility [7].

2. Hardware description

The telescope consists of a single arm with four detector planes as illustrated in fig. 1. A global right-handed coordinate frame is defined with the z axis in the direction of the beam and the y axis pointing upwards. This convention is adopted throughout this paper.

The detectors are mounted inside a custom hermetic enclosure to provide a cold, light-tight and humidity free environment. The top cover of this box was machined with slots to allow the insertion of detector planes with the use of matching flanges. The individual flanges are composed of matching half-moons which are attached to the detector boards for insertion in the slots. The positions of the telescope planes along the z axis are determined by predefined slots on the top cover, and are 0, 150, 250 and 290 mm. The

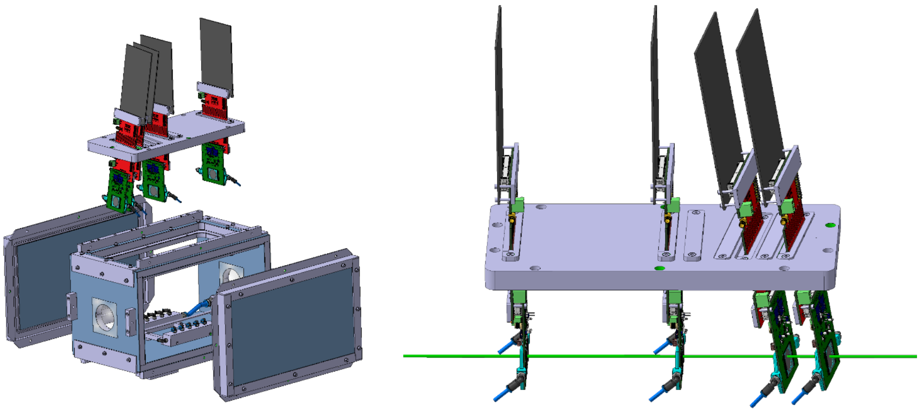

Figure 1: Mechanical design of the telescope-like arrangement of four measuring planes. The sensors are placed in a light-tight nitrogen environment, separated from the outside by flanges placed at predefined positions. The solid cylinder line cutting through the planes represents the traversing beam.

slots are machined to achieve different angles of the sensor planes with respect to the z axis. The two upstream sensors are perpendicular to the z axis to achieve a better temporal resolution. The other two sensors are angled at 9° with respect to the x and y axes in order to improve the spatial resolution [8]. For the majority of the data collection period, the first two slots were instrumented with 100 µm thick sensors (with identifiers N30 and N29), while 300 µm thick sensors (identified by N23 and N28) occupied the downstream slots. In the following sections, this is referred to as the default configuration. A limited data set was also acquired with an alternative configuration, where one 100 µm sensor (N29) was placed in an angled slot and a 300 µm sensor (N23) in the perpendicular slot. The base of the telescope box is mounted on a remote controlled motion stage, which allows the entire telescope to be moved along the x and y axes, to align the telescope with respect to the beam.

2.1. Timepix4 ASIC

Timepix4 is a readout ASIC capable of simultaneous time-of-arrival (ToA) and time-over-threshold (ToT) measurements [6]. The ASIC has a pixel matrix of 448×512 square pixels of 55 µm pitch. Hence, the total active area of the detector assemblies is around $24.6 \times 28.2\,\mathrm{mm}^2$. The ToA of each particle hit above a predefined and programmable threshold is measured by a time-to-digital converter (TDC) with a nominal bin width of 195 ps. Each group of 2×4 pixels, referred to as a superpixel, shares a Voltage Controlled Oscillator (VCO), which provides the 640 MHz reference clock for the pixel TDCs. For this beam test, version 1 of the Timepix4 (v1) was used, which has a flaw in the design of the VCO, causing it to oscillate about 25% too fast. For the same reason, the control voltage that is generated by the periphery Phase-Locked Loops (PLLs) could not be used, and hence the oscillation frequency was not stabilised, which negatively affects the time resolution[1]. The ToT measurements used in the analyses presented in this paper are performed with a 25 ns bin width.

The Timepix4 ASIC is divided into two halves, denoted top and bottom, in order to increase readout speeds by placing serialisers on both sides. The data can be read out by up to 16 serialisers capable of running at a maximum bandwidth of 10 Gbps each, to be capable of reading out a maximum hit rate of 3.6 Mhits/mm^2/s. During the beam test, only one serialiser per side was used, and the combined link speed was set to 2×2.56 Gbps, thereby limiting the bandwidth to order 100 Mhits/s, which is still about two orders of magnitude larger than the typical rate required for the H8 beam line.

2.2. Sensors

Planar n-on-p (electron collecting) silicon sensor technology is used in this system. The sensors are composed of p-type silicon bulk with n^+-type implants, and were manufactured by ADVACAM.[2] The back side is a uniform p^+ implant which is subsequently metallised to allow for the application of a reverse bias voltage to the sensor. The front side is segmented with 448×512 approximately 39 µm square n^+ implants, separated by a uniform p-spray, and covered with under bump metallisation which allows the pixels to be bonded with solder bumps to the ASICs. The 300 µm sensors are fully depleted at a reverse bias voltage of approximately 50 V with a leakage current of around 15 nA at room temperature, and they could be operated up to 150 V without breakdown. The 100 µm thick sensors are fully depleted at around 10 V with a leakage current of about 5 nA$atroomtemperature.Oneofthetwothinsensorspresentsbreakdownbelow$50 V, while the other could be reliably biased up to about 200 V. Two I-V characteristic curves of the 300 µm and 100 µm thick sensors are show in fig. 2.

---

[1] This design flaw is fixed in version 2 of the chip.

[2] Advacam, Tietotie 3, 02150 Espoo, Finland.

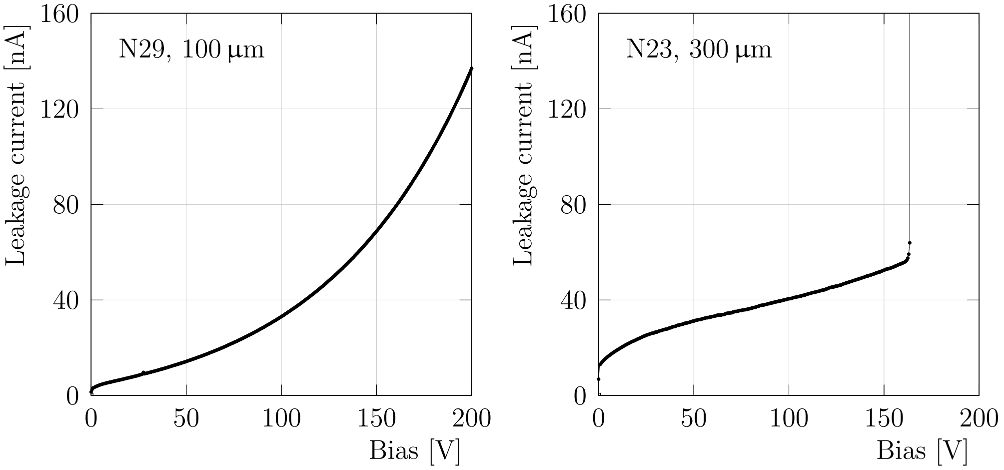

Figure 2: Left (Right): I-V characteristic curve for N29 (100 µm) and N23 (300 µm) sensors.

2.3. Cooling

Cooling of the planes is provided by a cooling block directly attached to the detector board, with a small surface overlap with the ASICs. The cooling blocks are made of 3D printed titanium with hollow cavities which allow liquid glycol to circulate through. The fluid is distributed in parallel to each of the planes. The cooling blocks have a circular cut-out to minimise the amount of material traversed by incident particles. The interface between the detector board and its cooling block was improved by attaching a high thermal conductivity sheet. The cooling fluid is pumped through the cooling block by an off-the-shelf chiller.

2.4. Scintillators

The timing measurements are complemented by three plastic (EJ100) scintillators mounted onto the telescope box. Two are placed upstream of the pixel sensors and spaced approximately 2 cm apart from each other, while the third is placed at the downstream side. The scintillators are instrumented with HPK[3] Photo Multiplier Tubes (PMTs) and their signals are processed by ORTEC-584 constant fraction discriminators (CFD) to minimise the contribution of timewalk to the electronics jitter. Each CFD output is fed back to

---

[3] Hamamatsu Photonics K.K., 325-6, Sunayama-cho, Naka-ku, Hamamatsu City, Shizuoka Pref., 430-8587, Japan.

a different Timepix4 plane where it is timestamped with a TDC of the same precision as that of the pixels. The synchronisation between the ASICs was found to be insufficiently stable to combine the three timestamps. The individual scintillators are all determined to have a resolution of around 100 ps, therefore the one most upstream was arbitrarily chosen to provide the reference time measurement.

3. Data acquisition

The Timepix4 ASICs are configured and read out with a custom developed system called SPIDR4, which is based on a Xilinx Zynq 7000 FPGA, provides the slow control interface to the Timepix4 via the on-chip ARM processor, which receives configuration commands via a 1 Gbit copper ethernet link. Regarding the slow control, all SPIDR4 systems are connected to the same computer, which runs four instances of the slow control application, one for each SPIDR4 plus Timepix4. Each instance of the DAQ (Data Acquisition) application is controlled by its corresponding slow control application. The main DAQ interface to the telescope is managed through a run-control application, which also directs all of the slow control instances.

The pixel data from Timepix4 consists of a 64 bit word for each hit. This hit data is transmitted from the chip to the FPGA using a serial 64/66 standard encoding scheme to allow for clock recovery and transmission line balancing. The distance between Timepix4 chip and FPGA is about 25 cm; the distance could be increased to about one meter, via commercially available FMC cables. The Timepix4 is operated with only one 2.56 Gbps serial link per half of the chip, as the track rates at this test beam were relatively low, typically below a million per second. The data from both links of each Timepix4 device are descrambled by the FPGA in SPIDR4 and packed into UDP datagrams, which are transmitted via an optical 10 Gbit ethernet connection to the DAQ computers, one for each SPIDR4. The main task of the DAQ application is to write the data to local disk, and no significant data processing is performed. The data are automatically copied to CERN's central file server system (EOS).

3.1. Software

A software application based on the Gaudi event processing framework [9], Kepler, has been developed for the reconstruction and analysis of data recorded with Timepix telescopes [2]. The core functionality of the software, which is to provide reconstructed and aligned tracks in a variety of formats to end users, remains largely unchanged. The main new feature in KEPLER is the implementation of a decoder for the Timepix4 data format. In addition, large improvements to the CPU performance of the reconstruction have been achieved by simplifying the intermediate data structures used by the software and modernisation of the code base.

3.2. Data quality monitoring

A new graphical user interface is implemented to control the execution of KEPLER and to monitor the quality of the collected data in real time, implemented using the QT5 toolkit. The communication between the interface and the KEPLER server is established through the Distributed Information Management (DIM) protocol [10]. The monitored information mostly consists of histograms of quantities such as the spatial and ToT distributions of the hits in each plane, as well as properties related to the clusters or tracks. In addition the number of errors in the configuration of the ASICs and in the data communication are displayed.

4. Experiment control system and monitoring

A dedicated experiment control system is implemented to remotely operate motion stages and power supplies, as well as to monitor the environmental conditions of the telescope. The system implementation is divided in the following way: the operation of High Voltage and the monitoring of bias currents (HV control); the operation of the motion stage (motion control); the monitoring of temperature and humidity. A block diagram representation of the system is given in fig. 3. The WinCC Open Architecture (OA) software suite (WinCCOA) is used to implement the control system, which also provides alarm and logging capabilities. The communication between WinCC OA and the hardware is established with a custom server based on the DIM protocol and the Open Platform Communications Unified Architecture (OPC UA).

The HV-control operates two Keithley 2410 Source Meters [4] that provide independent bias voltages to the 100 μm and 300 μm thick sensor planes in

---

[4] Tektronix, Inc. 14150 SW Karl Braun Drive, Beaverton, OR 97077. United States

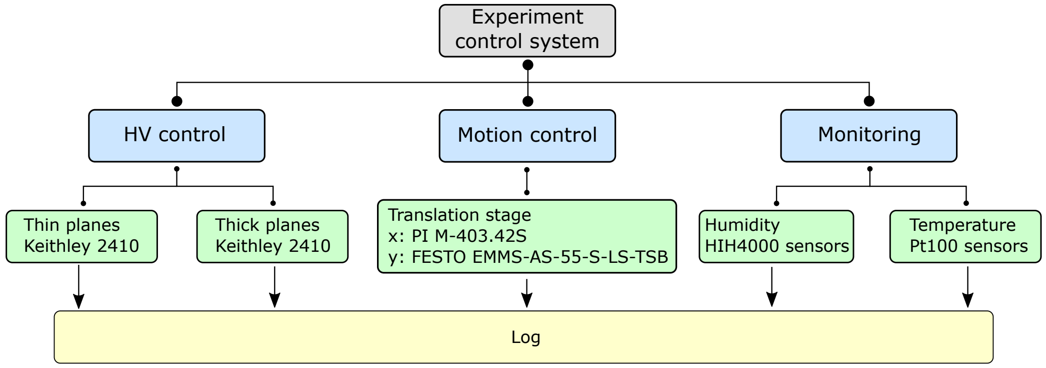

Figure 3: Schematic overview of the experiment control system.

the default configuration. The translation of the telescope along the x and y axes is performed by PI [5] motion stages with a repeatability of 2 µm.

The temperatures of each plane, as well as the temperature and humidity within the telescope enclosure, are monitored with four-wire Pt100 and HIH4000 sensors [6], connected via an Embedded Local Monitor Board (ELMB). The monitored values for each component are logged in order to enable studies of the telescope performance as a function of environmental conditions. In addition, the logging of operational settings such as the bias voltage complements the information manually recorded in the logbook of the testbeam.

5. Spatial resolution and efficiency

Clusters are reconstructed by grouping nearby hits that are within 100 ns from each other. The timestamp of the cluster is assigned as the earliest time measurement in the group of hits [3]. The cluster position is calculated as the ToT-weighted average of the position of the hits constituting the cluster. Particle tracks are reconstructed requiring a cluster in each plane and their trajectories determined using a straight line fit. The χ^2 of the track fit is required to be less than 40. The clusters are required to be within a 100 ns time interval allowing a low background and high-efficiency track reconstruction given the particle rate at the SPS was less than 2×10^5 particles/s. The

---

[5] Physik Instrumente (PI) GmbH & Co. KG Auf der Roemerstrasse 1 76228 , Karlsruhe, Germany

[6] Honeywell, Charlotte, North Carolina.

positions and orientations of the planes with respect to each other are determined using the Millepede algorithm [11], using a set of around 12,000 tracks. The alignment procedure is repeated several times, with progressively more stringent requirements on the χ^2 of the tracks in each iteration.

The residual is defined as the difference between the position of a cluster, and the extrapolated position of the track to the given plane. The residual is said to be *unbiased* if the cluster on the plane of interest is excluded from the track fit. The residuals are determined in the ASIC coordinate system where the x and y axes correspond to the directions of increasing column and row numbers, respectively. The resulting distributions are shown in fig. 4). The spatial resolution of each plane is defined as the RMS of the unbiased residuals. Clusters outside of a central interval containing 98.8% of the distribution are discarded before calculating the RMS, which is then referred to as the truncated RMS. The x residuals for the nominal data-taking conditions are shown in fig. 4. The truncated RMS is found, with negligible uncertainty, to be $33.2\,\mu\text{m}, 16.6\,\mu\text{m}, 7.2\,\mu\text{m}$ and $8.7\,\mu\text{m}$ for N30, N29, N23 and N28, respectively. The residual distribution is given by the convolution of the intrinsic resolution of the detector and the resolution of the track projection. The latter is the dominant contribution to the residual on the first plane due to the long extrapolation distance, and is estimated to be around $30\,\mu\text{m}$ from the track fit. The majority of clusters consist of a single hit for the $100\,\mu\text{m}$ planes placed perpendicular to the beam, which results in a worse resolution with respect to the angled planes. This can be seen from the characteristic top-hat distribution of N29 shown in the top right of fig. 4. The intrinsic resolution of the planes at their operating tilt is estimated from simulation, assuming that the resolution is equal in each direction and identical for planes with the same thickness and tilt. The resolutions are found to be $(15.5 \pm 0.5)\,\mu\text{m}$ for N30 and N29 and $(4.5 \pm 0.3)\,\mu\text{m}$ for N23 and N28, in agreement with the values found for tilted $300\,\mu\text{m}$ sensors bonded to Timepix3 [2]. The resolution is found to significantly degrade with increasing operating threshold, as can be seen in fig. 5. Conversely, the resolution is found to be largely independent of the applied bias voltage.

The single-plane efficiency is measured for each plane by reconstructing tracks from the other three planes and by searching for a cluster within $150\,\mu\text{m}$ and $100\,\text{ns}$ in space and time, respectively. The efficiencies are found to be $(92.0 \pm 5.0)\%$, $(99.4 \pm 0.2)\%$, $(99.1 \pm 0.4)\%$ and $(98.2 \pm 0.3)\%$ for planes N30, N29, N23 and N28, respectively. The uncertainties are assigned using run-to-run variations throughout the data taking period. The smaller

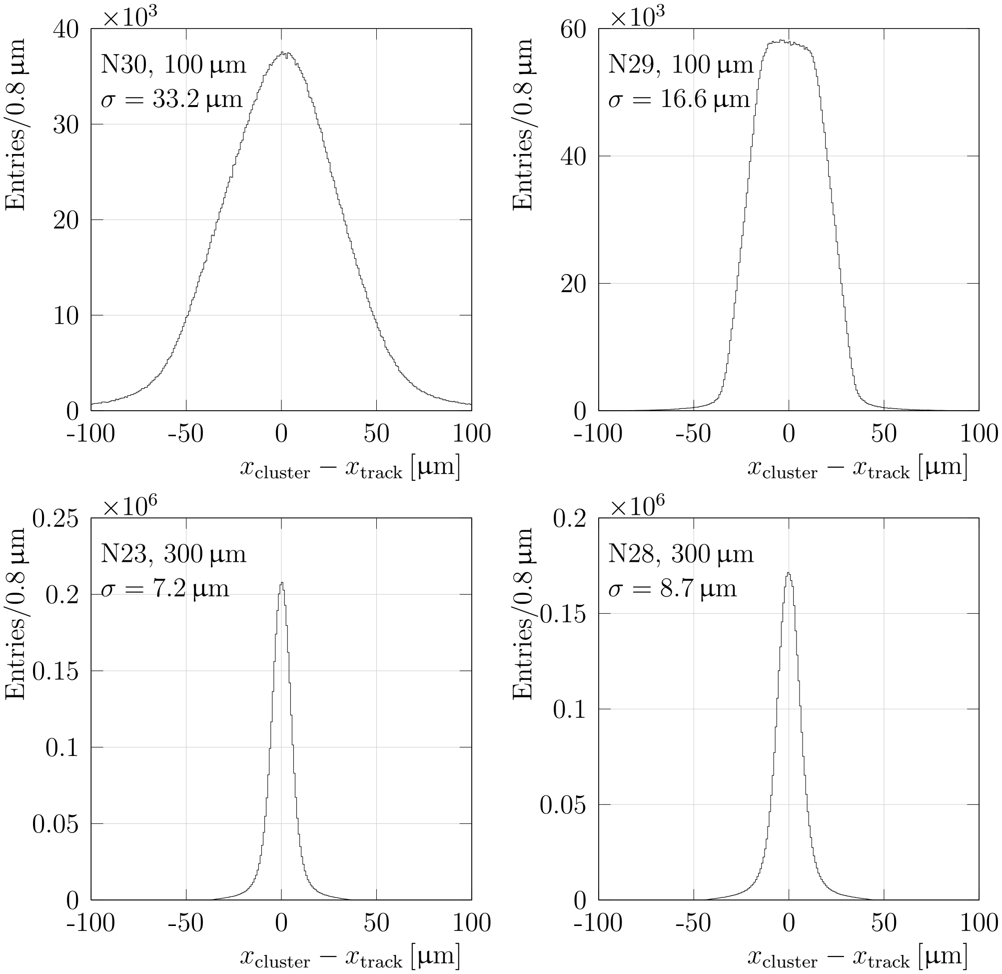

Figure 4: Distributions of x residuals for the clusters of each plane. The residual is defined as the difference between the cluster position and the intercept of the associated track.

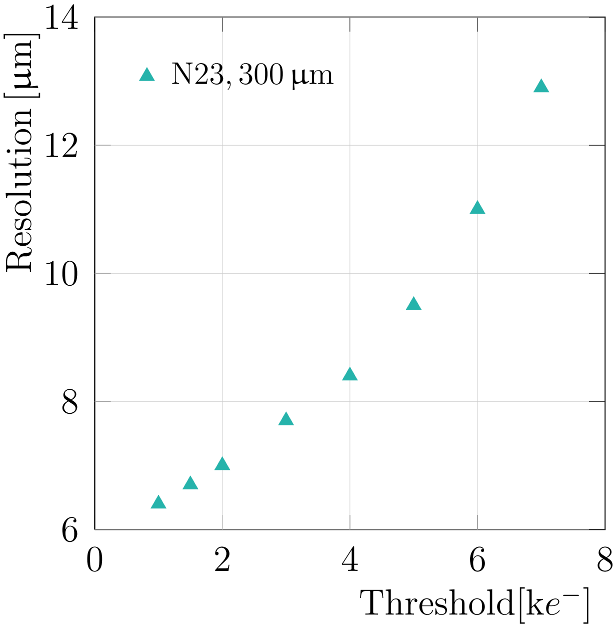

Figure 5: Resolution for the central 300 µm plane as a function of threshold.

efficiency and larger variation for plane N30 is due to a large number (around 10%) of malfunctioning columns.

6. Temporal performance

In this section, the temporal performance of each of the four Timepix4 planes is assessed. The time-to-threshold (TtT) is defined as the difference between the timestamp of the earliest hit in a cluster and the reference time. The time-to-threshold is analogous to the residuals for the spatial measurements, which yields the main figure-of-merit used in this section, the temporal resolution, defined as the RMS of the time-to-threshold distribution. The timestamps are corrected for timewalk and per-pixel time offsets. After applying these corrections, the resolution is studied as a function of bias and threshold.

Timewalk correction

It is important to correct for timewalk for low-amplitude signals, such as from the 100 µm sensors or for hits that share charge with other pixels in the same cluster in the 300 µm planes. The timewalk correction is performed based on the ToT of each hit, instead of the measured charge, since an accurate charge calibration procedure has not been developed for Timepix4 yet.

Two different timewalk correction methods are employed, depending on the angle of the sensor with respect to the beam, as described in [3]. For the perpendicular (100 μm) sensors, the timewalk correction is performed exclusively using the ToT of hits. A lookup table that contains the average TtT for each value of ToT is created per plane. An example timewalk distribution for N29 (100 μm) is shown in fig. 6 (top), where the line indicates the values in the lookup table. For the tilted (300 μm) sensors, the correction needs to account for timewalk and drift times, since the charge carriers can be liberated at different distances to the pixel implants [3].

The timewalk distribution for a tilted sensor is shown in fig. 6 (bottom). Multiple bands can be seen in the distribution, indicating the necessity of a correction that additionally accounts for the intrapixel track position at each plane. This method is described in detail in ref. [3]. Since this correction depends on drift velocity and threshold, the lookup table is determined for each set of operational settings.

Per-pixel corrections

A correction is required to account for per-pixel time offsets due to differences in VCO start time, and VCO frequency variations. The average TtT is determined for each pixel to account for these differences. Corrections for differences of the TDC bin sizes are not implemented due to the limited size of the data samples.

Figure 7 shows the average TtT of the pixels of N29 (100 μm), where the lines indicate the regions covered by the two upstream scintillators. The timestamps are corrected for timewalk before the average is determined for each pixel. The distribution of the average TtT of these pixels shows a large variation with an RMS of 315 ps. This effect is corrected by subtracting the average TtT of the pixel from the timestamp.

Time resolution

The four planes of the telescope are characterised as a function of the bias voltages and threshold. The temporal resolution is determined after both timewalk and per-pixel time offset corrections have been applied. Figure 8 shows the TtT distribution, before any correction (filled histogram), after the timewalk correction (hashed), and after both timewalk and per-pixel delay

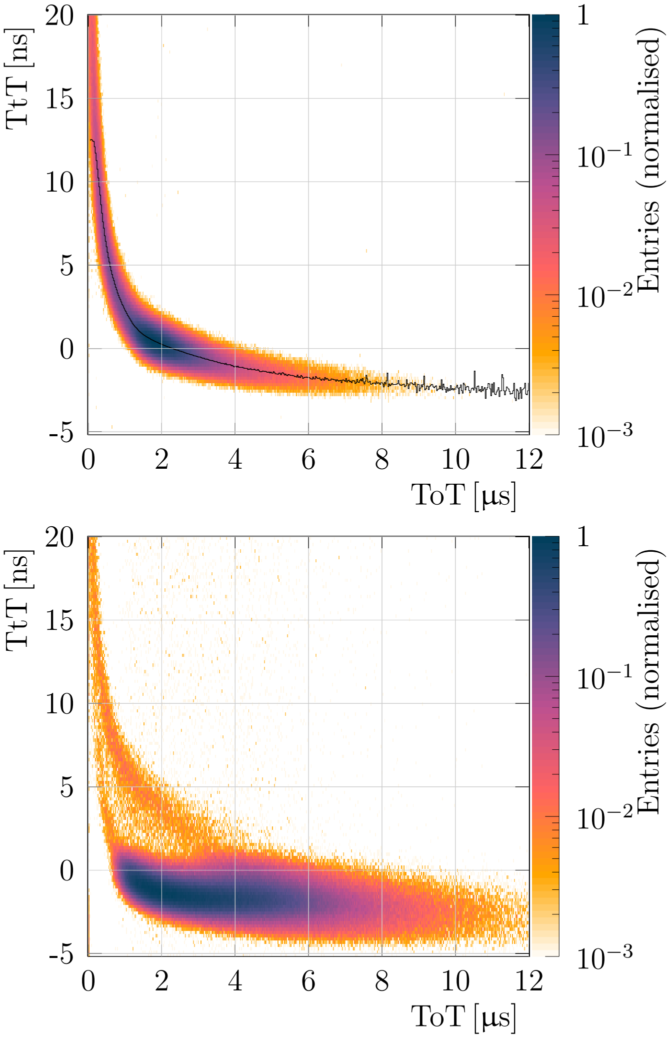

Figure 6: Top (bottom): Typical timewalk distribution for a 100 µm (300 µm) plane biased at 50 V (130 V). Since the 300 µm plane is tilted, the typical timewalk distribution shows multiple bands.

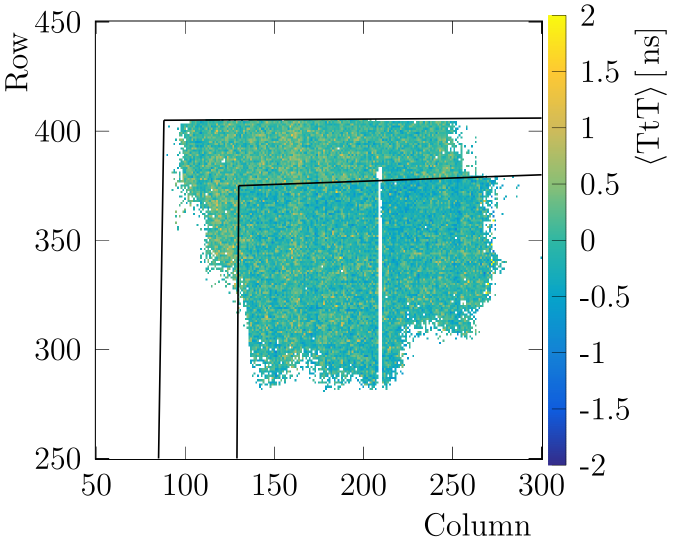

Figure 7: Measured average TtT of individual pixels of N29. The lines indicate the regions covered by each scintillator.

corrections (solid line). The time resolution is improved from (783 ± 24) ps to (439 ± 10) ps, implying that a total contribution of 648 ps has been removed.

The resolution changes as a function of operational settings such as bias voltage and threshold. Scans over these parameters are shown in fig. 9, where the left and right figures show bias and threshold scan, respectively. For all planes the time resolution shows improvement for higher bias voltages. The two tilted 300 µm sensors have a resolution that is significantly worse than that of the 100 µm sensors. The main cause is the more complex timewalk correction in addition to higher variations in the Ramo-Shockley weighting field, in comparison to the 100 µm sensors.

As shown in fig. 9 (right) the time resolution slightly improves as a function of threshold for the two 100 µm sensors, reaching the best resolution around the value of 2000 e^{-}. The two tilted 300 µm sensors do not show a local minimum. This is probably due to the larger variations in the time corrections. Plane N30 achieves its best resolution at 50 V, and the other planes at 130 V, all at a threshold of 1000 e^{-}. Their time resolutions are (452 ± 10) ps, (420 ± 10) ps, (639 ± 10) ps, and (631 ± 10) ps for N30, N29, N38, N23, respectively. The uncertainty is estimated from run-to-run variations.

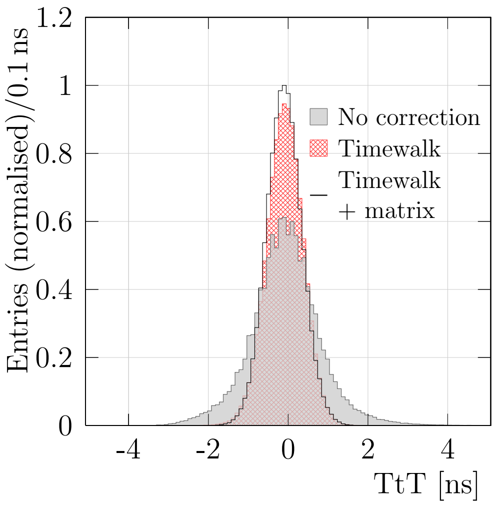

Figure 8: TtT distribution of all pixels of N29 (100 µm) biased at 50 V. The filled histogram indicates the uncorrected TtT distribution, the hashed represents this distribution after the timewalk correction, and the solid line displays this distribution after both a timewalk and per-pixel time offset correction.

The track time is determined by taking the uncertainty-weighted average of the individual measurements. To achieve the best track time resolution the planes should be biased at the highest operational high voltages. The resolution is determined in a configuration where the two thin planes are biased at 50 V and the other planes at 130 V, while the threshold is $1000\,e^-$ for all planes. The achieved track resolution is (340 ± 5) ps. The result of the combination of single plane measurements to a track is worse than what is expected from the naïve calculation using the separate resolutions. This is due to correlations between the time measurements, which can lead to a significantly worse resolution[3], and drift in the synchronisation between the planes.

7. Conclusions

A system composed of four Timepix4 detectors is used to reconstruct high energy hadrons from the CERN SPS H8 beam line. The overall spatial resolution is assessed for each of the detector planes by projecting the reconstructed tracks using the other three planes. The resolutions in the default configuration are estimated to be (15.5 ± 0.5) µm and (4.5 ± 0.3) µm for

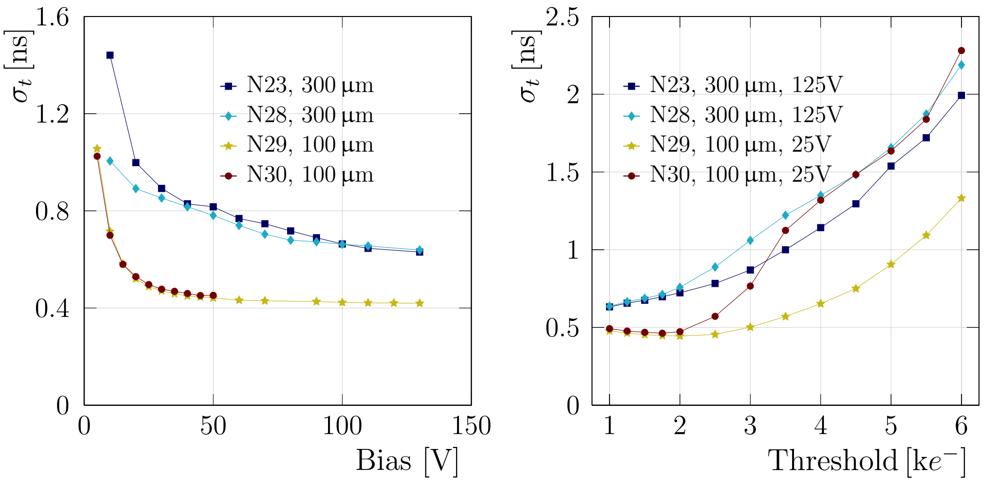

Figure 9: Left (right): time resolution of the four telescope planes as a function of the bias voltage (threshold). The four planes are indicated by the different markers.

100 µm and 300 µm thick sensors, respectively, after subtracting the expected contribution from the track extrapolation.

The timestamps from the detector are corrected for timewalk and per-pixel time offsets, finally yielding individual time resolutions of (452 ± 10) ps, (420 ± 10) ps, (639 ± 10) ps, and (631 ± 10) ps for N30, N29, N28, and N23, respectively, when compared to the measurements from the reference scintillators. These resolutions have been achieved at a threshold of $1000\,e^-$ and 50 V bias for N30, and 130 V for the other planes. These measurements can be combined to a track time resolution of (340 ± 5) ps.

8. Acknowledgements

We would like to express our gratitude to our colleagues in the CERN accelerator departments for the excellent performance of the beam in the SPS North Area. We gratefully acknowledge the support of the CERN Strategic R&D Programme on Technologies for Future Experiments[7] and the computing resources provided by CERN. We also gratefully acknowledge the support from the following national agencies: the Netherlands Organisation for Scientific Research (NWO); The Royal Society and the Science and Technology

---

[7] https://ep-rnd.web.cern.ch/

Facilities Council (U.K., grant no. ST/V003151/1 and ST/S000933/1); the European Research Council (grant no. 852642); the Wolfgang Gentner Programme of the German Federal Ministry of Education and Research (grant no. 13E18CHA); the German Federal Ministry of Education and Research (BMBF, grant no. 05H21PECL1) within ErUM-FSP T04; and the European Union's Horizon 2020 Research and Innovation programme (GA no. 101004761).

References

[1] K. Akiba, et al., Considerations for the VELO detector at the LHCb Upgrade II, LHCb Public Note: CERN-LHCb-PUB-2022-001 (Jan 2022). URL `http://cds.cern.ch/record/2800144`

[2] K. Akiba, et al., LHCb VELO Timepix3 Telescope, JINST 14 (05) (2019) P05026. `arXiv:1902.09755`, `doi:10.1088/1748-0221/14/05/P05026`.

[3] K. Heijhoff, et al., Timing performance of the LHCb VELO Timepix3 Telescope, JINST 15 (09) (2020) P09035. `arXiv:2008.04801`, `doi:10.1088/1748-0221/15/09/p09035`.

[4] K. Heijhoff, et al., Timing measurements with a 3D silicon sensor on Timepix3 in a 180 GeV/c hadron beam, JINST 16 (08) (2021) P08009. `arXiv:2105.11800`, `doi:10.1088/1748-0221/16/08/P08009`.

[5] E. Dall'Occo, et al., Temporal characterisation of silicon sensors on Timepix3 ASICs, JINST 16 (07) (2021) P07035. `arXiv:2102.06088`, `doi:10.1088/1748-0221/16/07/P07035`.

[6] X. Llopart, et al., Timepix4, a large area pixel detector readout chip which can be tiled on 4 sides providing sub-200 ps timestamp binning, JINST 17 (01) (2022) C01044. `doi:10.1088/1748-0221/17/01/c01044`.

[7] CERN Engineering Department. The H8 Secondary Beam Line of EHN1/SPS [online].

[8] E. Buchanan, et al., Spatial resolution and efficiency of prototype sensors for the LHCb VELO upgrade, JINST 17 (06) (2022) P06038. `arXiv:2201.12130v2`, `doi:10.1088/1748-0221/17/06/p06038`.

[9] M. Clemencic, et al., Recent developments in the LHCb software framework gaudi, Journal of Physics: Conference Series 219 (4) (2010) 042006. `doi:10.1088/1742-6596/219/4/042006`.

[10] C. Gaspar, M. Dönszelmann, P. Charpentier, DIM, a portable, light weight package for information publishing, data transfer and interprocess communication, Comput. Phys. Commun. 140 (2001) 102–109. `doi:10.1016/S0010-4655(01)00260-0`.

[11] V. Blobel, Software alignment for tracking detectors, Nucl. Instrum. Meth. A 566 (2006) 5–13. `doi:10.1016/j.nima.2006.05.157`.